Research Square

Preprints are preliminary reports that have not undergone peer review.
They should not be considered conclusive, used to inform clinical practice,
or referenced by the media as validated information.

Research on the Siting of Mother Stations for Dual-Purpose Mobile Charging Robots on Highways

Hao Jiang
Xinjiang University
Hailing Wang
Hailingwang@xju.edu.cn

Xinjiang University

Article

Keywords: Transportation Planning, Mobile Charging Robots, Facility Location Optimization, System Three-Stage Dynamic Location-Allocation Problem (STSDLAP), Dual-Use (Routine & Emergency)

Posted Date: April 2nd, 2026

DOI: https://doi.org/10.21203/rs.3.rs-8465872/v1

License: This work is licensed under a Creative Commons Attribution 4.0 International License.
Read Full License

Additional Declarations: No competing interests reported.

Research on the Siting of Mother Stations for Dual-Purpose Mobile Charging Robots on Highways

Hao Jiang，Hailing Wang*

Department of School of Economics and Management, Xinjiang University, Urumqi,830049，China.

*Corresponding author. E-mail: Hailingwang@xju.edu.cn;

Contributing authors: 464474309@qq.com;j464474309@163.com

ABSTRACT

To address the growing prominence of emergency charging rescue demands for electric vehicles on highways, as well as the issues of insufficient coverage from traditional fixed charging piles and inadequate emergency service capabilities, this paper proposes a methodology based on a System Three-Stage Dynamic Location-Allocation Problem (STSDLAP) for a dual-purpose (routine and emergency) mobile charging robot mother station system. First, Monte Carlo simulation is employed to predict the spatiotemporal distribution of both routine and emergency charging demands. Second, service capacity is evaluated based on non-preemptive priority M/M/C queuing theory to quantify waiting times and system load rates. Finally, an optimization model aiming to minimize cost and maximize coverage, while incorporating constraints on waiting time and load rate, is constructed and solved using the NSGA-II algorithm. Empirical results demonstrate that this solution can achieve emergency response within 30 minutes and meet over 95% of total charging demand on a 1000-kilometer highway section. Compared with traditional fixed charging pile solutions, it not only ensures daily service provision but also significantly enhances emergency handling efficiency. This study provides a reference for the flexible deployment of highway charging infrastructure and cost-effective emergency management.

Keywords: Transportation Planning; Mobile Charging Robots; Facility Location Optimization; System Three-Stage Dynamic Location-Allocation Problem (STSDLAP); Dual-Use (Routine & Emergency)

INTRODUCTION

Against the backdrop of "carbon peak" and "carbon neutrality" goals, the Electric Vehicle (EV), as a crucial green and clean alternative in the transportation sector, sees its charging infrastructure's rationality and service reliability directly impacting resource utilization and user experience. While fixed charging piles on highways may suffice for daily needs, they reveal significant shortcomings in emergency scenarios, such as slow response, insufficient coverage, and inflexible deployment. Consequently, there is an urgent need to establish a low-cost, high-coverage charging service mode that serves both "routine and emergency" purposes. The Mobile Charging Robot (MCR), with its flexible deployment and rapid response capabilities, effectively compensates for the coverage gaps of fixed infrastructure. Compared to the traditional tow-truck emergency rescue model, the MCR offers substantial advantages in response speed, user experience, and cost, presenting an innovative pathway to address the aforementioned challenges. However, systematic research on its dynamic siting is lacking. How to scientifically plan its dynamic deployment to achieve optimal resource allocation and efficient switching between routine and emergency scenarios has thus become a critical research problem. This study proposes the "System Three-Stage Dynamic Location-Allocation Problem (STSDLAP)" theory to address the complex challenges in siting MCR mother stations on highways for integrated routine and emergency operations.

The MCR mother station serves as the energy replenishment and dispatch base for the robots. It is selected and upgraded from existing fixed charging stations along the highway, thereby integrating with the fixed infrastructure to achieve the dual-purpose function. The MCRs can either leave the mother station to perform emergency rescue tasks or provide routine charging services within the station, alleviating pressure on fixed piles and ultimately delivering dual-purpose charging services for EVs. Compared to traditional tow-truck rescue, the MCR demonstrates significant advantages in responding to EV breakdowns due to power depletion on highways. It can arrive on-site for rapid energy replenishment within 30 minutes, reducing traffic disruption from hours to minutes, greatly enhancing rescue efficiency, and mitigating congestion and accident risks. User experience is notably improved, as drivers avoid prolonged waiting or vehicle towing, leading to greater safety and minimized trip interruption. From cost and investment perspectives, the MCR's direct service cost per instance is lower. Furthermore, functioning as a "mobile energy storage unit," it enables intelligent dispatch, higher asset utilization, and the flexibility of "dual-use" to dynamically balance charging demands. MCRs provide dynamic cyclic services across the road network, utilizing interchanges to change travel direction, thereby maintaining a dynamic balance in the number of MCRs at each mother station. After replenishing a stranded EV, to prevent the MCR itself from running out of power on the highway, it must return to a mother station for its own recharge and continue circulating for work among the network of stations. Therefore, the scientific layout of mother station locations is essential to reduce MCR operational costs and improve their service coverage. The STSDLAP theoretical framework encompasses key elements such as infrastructure, operational service equipment, information transmission, energy exchange, and service vehicles, collectively forming a three-stage dynamic system.

In the field of collaborative planning for charging infrastructure, existing research has shown a trend evolving from single-mode systems towards hybrid "fixed-mobile" models. Hu Dandan et al. [1] explored hybrid layouts of battery swapping and charging via gas station retrofits, while Zhang Meixia et al. [2] and Li et al. [3]deepened this approach from perspectives of bi-level programming and integration, respectively. With increasing demand for service flexibility, Liu et al. [4]and Hua et al. [5] further introduced mobile charging units, constructing three-tier networks or asset-light models. The O2O system proposed by Tang et al. [6] represents the latest progress in dispatch intelligence. However, these existing models are optimized for urban scenarios and are difficult to apply to the closed, linear, long-distance, and emergency-prone context of highways. In the highway environment, the coordinated dispatch of MCRs and fixed charging piles faces the dual challenge of optimizing resource allocation while ensuring service quality and controlling the system load rate to prevent overload and paralysis. To address this, this study constructs a dynamic feedback model that

interlinks core elements such as mother station locations, the number of charging piles, and the number of robots. This model aims to achieve optimal collaborative dispatch under the constraints of meeting service quality requirements and system load limits.

Accurate prediction of charging demand is the foundation of facility planning. Existing research in this area has formed multiple technical pathways ranging from behavioral analysis and data mining to dynamic modeling. Yang Yazan et al. [7]constructed prediction models based on the charging behavior characteristics of multiple vehicle types; Cao Mukun et al. [8] mined demand points relying on a trajectory data-driven paradigm; Jiang Changxu et al. [9] further considered inter-station interaction influences to build a dynamic demand model; Chowdhury et al. [10] proposed a "Mobile Charging Station Allocation Index" (MCSAI) combined with dynamic fault tree analysis to predict time-slot-specific demand. These methods are suitable for urban scenarios but do not fully account for emergency demands triggered by events like battery depletion on highways. Moreover, they often treat energy consumption per unit distance as a fixed value. On highways, vehicle energy consumption is significantly affected by rolling resistance, aerodynamic drag, and intermittent congestion. Simplified models would lead to deviations in predicting driving range and demand points. Therefore, this study proposes a prediction method that integrates an EV energy consumption model, a travel behavior model, and Monte Carlo simulation. This approach authentically reflects the energy consumption patterns of highway vehicles and generates both routine and emergency demand data, providing reliable support for subsequent planning and dispatch.

In charging facility planning, accurately evaluating service performance is a key link for optimizing resource allocation. In this area, Dai Yang et al. [11] introduced path feasibility and multi-server queuing theory for inter-city travel scenarios; Shi Ruifeng et al. [12]directly applied the M/M/N/FCFS model to calculate EV waiting times and queue lengths; Zhang Wenhui et al. [13] and Wang et al. [14] both used queuing theory models to constrain service intensity or reduce user waiting times. Existing studies treat charging demands as homogeneous entities, following a "first-come, first-served" principle, which cannot guarantee priority service for emergency charging demands when resources are limited. To address this, this study introduces an M/M/C non-preemptive priority queuing model to improve the service performance evaluation method. This more realistically reflects the service quality of highway charging facilities under the "integrated routine and emergency" mode, providing more precise service constraints for subsequent resource optimization.

In the decision-making stage of charging facility planning, location-sizing models are decisive for the feasibility and operational efficiency of proposed solutions. Yang Jieqing et al. [15] focused on economic viability and suitability; Liu Hong et al. [16] balanced operator costs and user waiting times; Zhang Zhaolei et al. [17] emphasized the overall charging service efficiency of the system. Additionally, Cui et al. [18]and Liu et al. [19] performed optimizations from the perspectives of multi-mode service trade-offs and driver psychological behavior, respectively. A diverse toolbox of algorithms has also been formed. For instance, Li Jiapei et al. [20] applied a bi-objective label-setting method and branch-and-bound; Li Jianxia et al. [21]used HOMER software and tabu search; Ge Shaoyun et al.[22] introduced the VIKOR method for multi-attribute decision-making; while Kaya et al. [23]performed optimization through a Mixed Integer Programming (MIP) framework. Existing models and algorithms target single, routine scenarios and struggle to adapt to the dual requirements of the highway "dual-use" strategy: cost control and emergency service reliability. Therefore, this study combines a Maximum Coverage model to construct a multi-objective optimization model tailored for this scenario, incorporating waiting time constraints and system load rate thresholds. For the solution method, an improved genetic algorithm is selected to achieve efficient and stable optimal solutions.

1 System Three-Stage Dynamic Planning Theory

The core of the STSDLAP lies in the dynamic coupling and closed-loop feedback among its three stages. Each stage sequentially connects to the next, where the output of a preceding stage serves as the input for the following one. Simultaneously, optimization results are fed back to earlier stages, forming a closed loop. This framework achieves holistic system

optimization through a dynamic feedback mechanism and transfer functions.

1.1Dynamic Feedback Model

The system employs a time-based feedback loop, where the optimization decisions from the third stage influence the charging demand prediction in the first stage and the dispatch strategy in the second stage. The feedback model enables system adaptation through the update of state variables. Mathematically, the system state vector can be represented as:

$$X(t)=\left[\mathrm{D}(t),\mathrm{W}(t),\rho(t),\mathrm{Y}(t),\mathrm{K}_r(t),\mathrm{K}_c(t)\right] \quad (1\text{-}1)$$

Where:

$\mathrm{D}(t)$ represents the spatiotemporal distribution of charging demand.

$\mathrm{W}(t)$ denotes the average user waiting time.

$\rho(t)$ signifies the system load rate.

$\mathrm{Y}(t)$ is the mother station location decision vector.

$\mathrm{K}_r(t)$ is the number of MCRs.

$\mathrm{K}_c(t)$ is the number of fixed charging piles.

System dynamics are described by the state equation:

$$X(t+1)=f\left(\mathrm{X}(t),\mathrm{U}(t)\right) \quad (1\text{-}2)$$

Here, $\mathrm{U}(t)$ represents external inputs such as traffic flow and random incidents, and f is a nonlinear function encompassing the relationships among the three stages.

1.2 Transfer Functions

Transfer Function for Stage 1:This converts traffic data into charging demand prediction. Let traffic flow be $\mathrm{F}(t,x)$, and the probability of random incidents be $P(t)$, The demand prediction model is:

$$D(t,x)=f_1\left(\mathrm{F}(t,x),P(t),\theta_1\right) \quad (1\text{-}3)$$

Here, f_1 integrates the EV travel model and Monte Carlo simulation, and θ_1 represents model parameters such as vehicle energy consumption and battery capacity. The output $\mathrm{D}(t,x)$ is a spatiotemporal demand matrix.

Transfer Function for Stage 2: This transforms demand input into service performance metrics. Based on M/M/C queuing theory and non-preemptive priority dispatch (giving priority to emergency demand), the service model is:

$$\left[W_{\mathrm{n}}(t),\rho(t)\right]=f_2\left(\mathrm{D}(t),\mu,K_r(t),K_c(t),\theta_2\right) \quad (1\text{-}4)$$

Where f_2 encapsulates the queuing model, μ is the service rate, and θ_2 are dispatch parameters. The outputs $W_{\mathrm{n}}(t)$ and $\rho(t)$ are in vector form, representing the service metrics for each mother station.

Transfer Function for Stage 3:This converts service metrics and cost data into optimization decisions. The multi-objective optimization model is:

$$minC\left(\mathrm{Y},K_r,K_c\right),maxQ\left(\mathrm{Y},K_r,K_c\right) \quad (1\text{-}5)$$

Subject to constraints: $\mathrm{W}\le W_{\max}$, $\rho\le\rho_{\max}$, etc. The transfer function is solved using an improved NSGA-II algorithm, outputting the optimal configuration Y^*,K_r^*,K_c^*.

2 Charging Demand Prediction Based on Monte Carlo Simulation

2.1 EV Energy Consumption Model

This study focuses on flat highway segments, primarily considering three core factors: rolling resistance, aerodynamic drag, and traffic congestion. The influence of other factors such as road gradient and climate variations is temporarily excluded. The energy consumption

model is based on the physical principles of constant-speed vehicle travel, decomposing the energy consumption per unit distance into two components: baseline rolling energy consumption and aerodynamic drag energy consumption. A congestion factor, $f_{congestion}$ (where $f_{congestion} \geq 1$), is introduced to comprehensively reflect additional energy losses caused by traffic flow variations, such as congestion, sudden acceleration, and sudden deceleration.

Assumption 1: The fundamental physical formulas are most accurate when the vehicle maintains a constant speed.

Assumption 2: The model is suitable for average energy consumption prediction at the road segment level, not for instantaneous second-by-second calculation.

Assumption 3: The complex effects of non-uniform speed are aggregated into an average speed-related correction factor.

1.Baseline Rolling Energy Consumption

$$e_{rolling} = \frac{\mu_{roll} \cdot m \cdot g}{3600} \quad (2\text{-}1)$$

Where, $e_{rolling}$ represents the rolling energy consumption per unit distance, μ_{roll} is the rolling resistance coefficient (e.g., Wh/km), m is the total vehicle mass (kg), g is the gravitational acceleration (m/s²).

2.Aerodynamic Drag Energy Consumption

$$e_{air} = \frac{0.5 \cdot \rho_{air} \cdot C_d \cdot A \cdot (v_{/3.6})^2}{3600} \quad (2\text{-}2)$$

Where e_{air} is the aerodynamic drag energy consumption per unit distance (Wh/km), ρ_{air} is the air density (kg/m³), C_d is the drag coefficient, A is the vehicle frontal area (m²), and v is the EV travel speed (m/s).

3.Congestion-induced Additional Energy Consumption

Traffic congestion causes frequent acceleration and deceleration, preventing vehicles from maintaining an economical speed. The acceleration process consumes significant kinetic energy, while braking dissipates most of this energy as heat, with regenerative braking systems only recovering a portion. These frequent, small-amplitude speed fluctuations, even if the average speed remains constant (e.g., 105 km/h), introduce additional kinetic energy losses not captured by an ideal constant-speed model. The physical meaning of the congestion $f_{congestion}$ lies in quantifying the extra energy cost required to maintain a dynamic average speed compared to maintaining a static constant speed. This study assumes $f_{congestion} \approx 1.2$.

4.Total EV Energy Consumption

$$G_V = \left(e_{rolling} + e_{air}\right) \times f_{congestion} \quad (2\text{-}3)$$

Where G_V is the energy consumption per unit distance for the EV (Wh/km).

2.2 EV Travel Model

The study categorizes battery electric vehicles (BEVs) into three clusters based on battery capacity: F_{V1}, F_{V2} and F_{V3}.For each battery capacity category, vehicles are further divided into two body types: sedans and SUVs.

Assumption 1: Under the conditions of the aforementioned energy consumption model, the travel distance of an EV is positively correlated with its battery capacity F_V.

Assumption 2: The charging efficiency is assumed identical for both emergency and routine demand. Different vehicle types share a unified distribution for the charging trigger threshold. A routine charging demand is generated when the vehicle's State of Charge (SOC) falls below this threshold. The location, required energy, remaining travelable distance, and other parameters are recorded.

Assumption 3: A portion of the routine demands are randomly designated as emergency demands through a Bernoulli trial, based on the probability proportional to the traffic flow ratio in the current time period[24]. Depending on their type, both demands are served either by

an MCR or a fixed charging pile, charged to a target $S_{soc,o}$ before resuming travel. The specific formulas are as follows:

$$D_e = \frac{\eta_t \left(S_{soc,e} - S_{soc,c}\right) F_V}{G_V} \quad (2\text{-}4)$$

$$D_c = \frac{\eta_t S_{soc,c} F_V}{G_V} \quad (2\text{-}5)$$

$$T_e = \frac{E_e}{P_e \eta_c} \quad (2\text{-}6)$$

$$T_n = \frac{E_n}{P_n \eta_c} \quad (2\text{-}7)$$

$$P = \frac{q_{current}}{Q_{total}} \quad (2\text{-}8)$$

Where:

$S_{soc,e}$, $S_{soc,c}$, $S_{soc,o}$ are the initial SOC upon highway entry, the SOC threshold triggering charging demand, and the target SOC after charging, respectively.

D_e, D_c are the travel distance from the entry point to reaching the charging threshold and the remaining travelable distance after reaching the threshold, respectively.

η_t is the battery-to-wheel energy conversion efficiency.

η_c is the charging efficiency.

G_V is the energy consumption per km (kWh/km).

T_e, T_n are the charging durations for emergency and routine services.

P_e, P_n are the charging powers for emergency and routine services.

E_e, E_n are the energy demands per emergency and routine charging session.

P is the probability of a routine demand being converted to an emergency demand, $q_{current}$ is the traffic flow in the current time slot, and Q_{total} is the total daily traffic flow.

2.3 Monte Carlo Simulation Model

Building upon the above, a Monte Carlo simulation is employed to predict the spatiotemporal distribution of EV charging demand. The detailed flowchart is shown in **Figure 1**, and the specific steps are as follows:

Step 1. Import data including highway segment distances, time-series traffic flow, and vehicle parameters.

Step 2. Randomly generate six different types of vehicles via Monte Carlo simulation. For the nth EV, read its corresponding departure time, vehicle type, etc. Randomly generate the vehicle's initial State of Charge (SOC), charging threshold, travel speed, and other parameters. Dynamically predict the EV's per-unit-distance energy consumption using the EV energy consumption model.

Step 3. During the EV's travel, continuously update the vehicle's SOC based on its initial SOC, per-unit-distance energy consumption, and travel speed. When the vehicle's SOC drops below the charging threshold, a routine charging demand is generated. Key indicators such as location, time, and energy demand are recorded, and the vehicle's state is updated.

Step 4. Based on the vehicle's departure time and the corresponding time slot's traffic flow, calculate the probability of emergency demand conversion. Determine whether this demand point should be designated as an emergency demand.

Step 5. Perform K-Means clustering on the detailed list of obtained charging demands. The final output is the spatiotemporal distribution of EV charging demands on the highway.

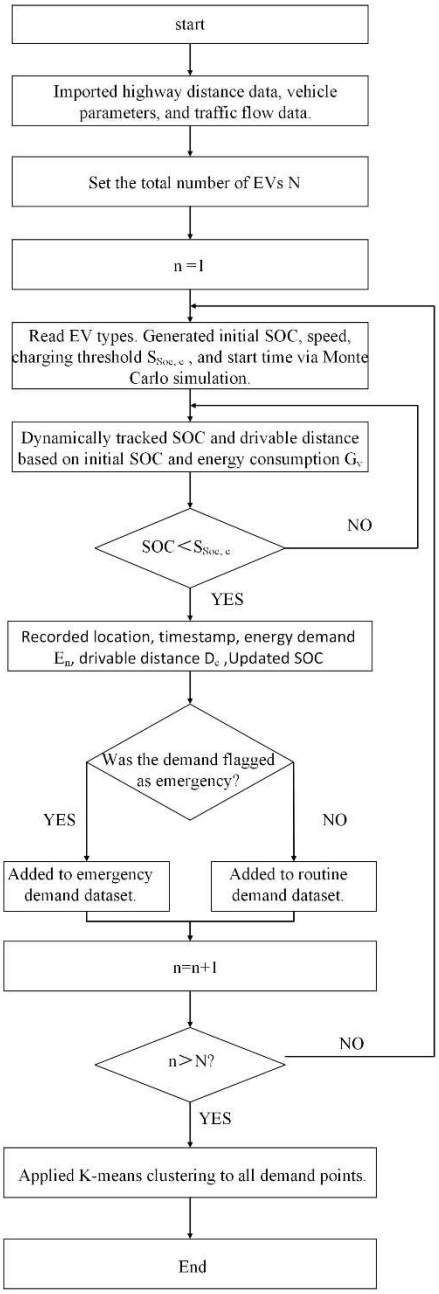


Figure 1 Flowchart of charging demand prediction

3 M/M/C Queuing Theory Model

3.1 System Description and Model Assumptions

To accommodate the efficient switching between routine and emergency scenarios for charging piles and MCRs, a non-preemptive priority queuing model is employed. The process of EVs arriving at a mother station or remotely issuing emergency requests is assumed to be independent, stationary, and possessing no aftereffects, thus modeled as a Poisson process[25]. To reflect the relative importance between different priority classes, a priority factor α is introduced into the formulas for calculating system performance metrics as a quantitative weight.

Assumption 1. Server Configuration: Each mother station is equipped with k_r MCRs and

k_c fixed charging piles. The MCRs can travel to emergency demand points for service or serve routine demands within the station. Their battery capacity is F_r, travel speed is v_r,and energy consumption per unit distance is G_r,Fixed piles are for in-station use only.

Assumption 2. Request Classification: Charging requests are categorized into two classes:

Type I (Emergency Request): High priority, following a Poisson arrival process with parameter λ_1.

Type II (Routine Request): Low priority, following a Poisson arrival process with parameter λ_2.

Assumption 3. Service Discipline:Routine requests are primarily served by fixed piles; MCRs are utilized when fixed piles are insufficient. Emergency requests are handled with a non-preemptive priority dispatch policy, meaning ongoing routine services are not interrupted. MCR resources are dynamically allocated based on the emergency load.

Assumption 4. Travel Time: The MCR travel time τ from the station to a demand point follows a deterministic distribution, calculated based on road distance and speed.

3.2 Mathematical Model Formulation

The process of EVs receiving service at a mother station follows a Poisson distribution with parameter λ, where λ_e and λ_n represent the arrival rates (frequency per unit time) for emergency and routine charging applications, respectively.

A mother station is equipped with k_r homogeneous MCRs and k_c homogeneous fixed charging piles. The service time for each device is independent and follows a negative exponential distribution with parameter μ. Here, μ_e and μ_n correspond to the service rates for emergency and routine demands, respectively. A priority factor α is introduced into the model to increase the weight of emergency service capacity in the calculations. The formulas are as follows:

$$\mu_e = \frac{1}{T_e} = \frac{P_e \eta_c}{E_e}(1+\alpha) \quad (2\text{-}9)$$

$$\mu_n = \frac{1}{T_n} = \frac{P_n \eta_c}{E_n}(1-\alpha) \quad (2\text{-}10)$$

As the mother station is a dynamic system, the operation of MCRs and charging piles must not exceed the system's capacity. Let ρ_e denote the load rate for emergency demand, and ρ_n^{charge} and ρ_n^{robot} represent the load rates for the fixed piles and MCRs serving routine demand, respectively. k_r^{eff} denotes the effective number of MCRs available. The formulas are:

$$\rho_e = \frac{\lambda_e}{k \cdot \mu_e} \quad (2\text{-}11)$$

$$\rho_n^{charge} = \frac{\lambda_n}{k_c \cdot \mu_n} \quad (2\text{-}12)$$

$$\rho_n^{robot} = \frac{\lambda_n}{k_r^{eff} \cdot \mu_n} \quad (2\text{-}13)$$

$$k_r^{eff} = k_r \cdot \left(1 - min\left(\rho_e, 1.0\right)\right) \quad (2\text{-}14)$$

W_e represents the waiting time for emergency demand, including queuing time for charging and MCR travel time. W_n represents the waiting time for routine demand, which includes only the queuing time for charging. d_i denotes the distance from the station to demand point i. S_e and S_n represent the expected residual service times for emergency and routine requests, respectively. v_r is the travel speed of the MCR. The formulas are:

Queuing Time for Emergency Requests:

$$W_{q,e} = \frac{R}{1-\rho_e} \quad (2\text{-}15)$$

Expected Residual Service Time:s

$$R = \frac{1}{2}\left(\lambda_e E\left[S_e^2\right] + \lambda_n E\left[S_n^2\right]\right) \quad (2\text{-}16)$$

Second Moment of Service Time (Exponential Distribution):

$$E\left[S_e^2\right] = \frac{2}{\mu_e^2} \quad (2\text{-}17)$$

$$E\left[S_n^2\right] = \frac{2}{\mu_n^2} \quad (2\text{-}18)$$

Travel Time:

$$t_m = \frac{1}{I}\sum_{i=1}^{I}\frac{d_i}{v_r} \quad (2\text{-}19)$$

Total Waiting Time for Emergency Request:

$$W_e = W_{q,e} + t_m \quad (2\text{-}20)$$

Idle Probability for Fixed Pile System:

$$P_0^{charge} = \left[\sum_{q=0}^{k_c-1}\frac{\left(k_c\rho_n\right)^q}{q!} + \frac{\left(k_c\rho_n\right)^{k_c}}{k_c!\left(1-\rho_n\right)}\right]^{-1} \quad (2\text{-}21)$$

Probability All Fixed Piles are Busy:

$$P_{\text{busy}}^{charge} = \frac{\left(k_c\rho_n\right)^{k_c}}{k_c!}\cdot\frac{P_0}{\left(1-\rho_n\right)} \quad (2\text{-}22)$$

Queuing Time for Routine Requests at Fixed Piles:

$$W_{q,n}^{charge} = \frac{P_{\text{busy}}^{charge}}{k_c\mu_n - \lambda_n} \quad (2\text{-}23)$$

Idle Probability for MCR System (serving routine demand):

$$P_0^{robot} = \left[\sum_{q=0}^{k_r-1}\frac{\left(k_r\rho_n\right)^q}{q!} + \frac{\left(k_r\rho_n\right)^{k_r}}{k_r!\left(1-\rho_n\right)}\right]^{-1} \quad (2\text{-}24)$$

Probability All Available MCRs are Busy:

$$P_{\text{busy}}^{robot} = \frac{\left(k_r\rho_n\right)^{k_r}}{k_r!}\cdot\frac{P_0}{\left(1-\rho_n\right)} \quad (2\text{-}25)$$

Queuing Time for Routine Requests at MCRs:

$$W_{q,n}^{robot} = \frac{P_{\text{busy}}^{robot}}{k_r^{eff}\mu_n - \lambda_n} \quad (2\text{-}26)$$

Total Waiting Time for Routine Request:

$$W_n = \begin{cases} W_{q,n}^{charge} & if\ \rho_n^{charger} < 1 \\ W_{q,n}^{robot} & otherwise \end{cases} \quad (2\text{-}27)$$

4 Multi-Objective Optimization Model for Siting Dual-Use MCR Mother Stations

4.1Objective Function Formulation

The siting problem in this study aims to maximize charging demand coverage under limited resource constraints. Therefore, the Maximum Coverage Model (MCM) is adapted to address the siting problem. Considering the real-world scenario, the highway is treated as a one-dimensional network. Interchanges between the two directional carriageways allow MCRs to change direction, but reversing on the highway is prohibited. Each EV can select only one final servicing mother station. MCRs operate in a dynamic cycle within the network, utilizing interchanges to switch directions to maintain a dynamic balance in the number of robots at each mother station. After replenishing a stranded EV, to prevent the MCR itself from running out of power on the highway, it must proceed to a mother station for its own recharge and continue circulating among stations. Therefore, for an emergency charging demand, it is considered covered if an MCR can be dispatched from an upstream mother station, and after servicing, the MCR has sufficient remaining charge to reach the next designated mother station for its own replenishment. For a routine charging demand, it is considered coverable by a station if the EV's remaining charge is sufficient to reach that station.

Integrating the Maximum Coverage Model, a multi-objective optimization model is established. The optimization objectives are to minimize the total annualized cost and to maximize the charging demand coverage rate. The total cost includes mother station construction, MCR and charging pile procurement, as well as related operation and maintenance costs. Costs associated with empty mileage, additional energy consumption, and time occupancy for MCRs are not considered in this study.

The objective functions are as follows:

（1）Annualized Construction, Operation, and Maintenance Cost:

$$minC = c_{fix} + c_{rc} + c_{OPEX} \quad (3\text{-}1)$$

$$\delta = \frac{\beta(1+\beta)^T}{(1+\beta)^T - 1} \quad (3\text{-}2)$$

Where Y_m , K_{rm} , K_{cm} are the decision variables for mother station establishment, number of MCRs, and number of fixed charging piles at candidate site m , respectively. δ is the capital recovery factor, used to convert the present value P into an equivalent uniform annual value A over a planning horizon of $T = 20$ years, with a discount rate β of 0.1.

A. Annualized Mother Station Construction Investment Cost

$$c_{fix} = \delta \sum_{m=1}^{N_c} Y_m c_{cs,m} \quad (3\text{-}3)$$

Where $c_{cs,m}$ is the fixed cost for establishing a mother station at candidate site m , primarily including station construction costs, transformer and power supply equipment costs, and MCR/charging pile maintenance equipment costs. $Y_m = 1$ if a station is built at site m , otherwise $Y_m = 0$. N_c is the total number of candidate sites.

B. Annualized MCR and Charging Pile Procurement Cost

$$c_{rc} = \delta \left(\sum_{m=1}^{N_c} K_{rm} Y_m c_r + \sum_{m=1}^{N_c} K_{cm} Y_m c_c \right) \quad (3\text{-}4)$$

Where c_r is the unit price of an MCR, and c_c is the unit price of a charging pile. The procurement cost is calculated based on the quantities of MCRs and charging piles.

C. Annual Operation and Maintenance Cost for MCRs and Charging Piles

$$c_{OPEX} = \theta \delta \sum_{m=1}^{N_c} Y_m K_m c_{cs,m} \quad (3\text{-}5)$$

Where θ is a conversion coefficient used to estimate the annual operation and maintenance cost per unit of MCR or charging pile based on its investment cost. This mainly includes expenses for electricity consumption, personnel salaries, inspection, and

maintenance.

（2）Charging Demand Coverage Rate

To reflect the differentiated service of mother stations for routine and emergency charging demands, a priority factor α is introduced into the maximum coverage objective function, assigning higher weight to emergency demands. The specific formula is:

$$maxQ = (1+\alpha)\sum_{i\in I} Z_i + (1-\alpha)\sum_{j\in J} W_j \quad (3\text{-}6)$$

Where:

Z_i indicates whether emergency demand point i is covered by an upstream mother station. $Z_i = 1$ if covered, otherwise 0.

W_j indicates whether routine demand point j is covered by a downstream mother station. $W_j = 1$ if covered, otherwise 0.

4.2 Constraints

（1）MCR and Charging Pile Quantity Constraints

To ensure the basic service capability of a mother station, the number of MCRs and charging piles at established stations is bounded:

$$K_{rmin} \le K_{rm} \le K_{rmax} \quad (3\text{-}7)$$

$$K_{cmin} \le K_{cm} \le K_{cmax} \quad (3\text{-}8)$$

Where K_{rmin} and K_{cmin} are the minimum required numbers of MCRs and charging piles to guarantee basic service capacity. K_{rmax} and K_{cmax} are the maximum allowable numbers to prevent resource wastage from over-deployment.

（2）Logical Constraints between Station and Devices

To ensure consistency between station establishment and device deployment:

$$K_{rm} \le K_{rm} \cdot Y_m \quad (3\text{-}9)$$

$$K_{cm} \le K_{cm} \cdot Y_m \quad (3\text{-}10)$$

Where, This enforces that if $Y_m = 0$ (no station), then K_{rm} and K_{cm} must be 0. If $Y_m = 1$, then K_{rm} and K_{cm} can be greater than 0.

（3）Load Rate Constraints

To ensure rapid response capability for emergency demands and overall system stability, constraints are imposed on the emergency load rate and the total system load rate:

$$\rho_e \le \rho_{max} \quad (3\text{-}11)$$

$$\rho_n^{robot} \le \rho_{max} \quad (3\text{-}12)$$

$$\rho_n^{charge} \le \rho_{max} \quad (3\text{-}13)$$

Where ρ_{max} is the maximum allowable load rate for emergency demand to guarantee fast response. ρ_n^{robot} and ρ_n^{charge} are the maximum load rate limits for fixed piles and MCRs serving routine demand, respectively, calculated according to Section 3.2.

（4）Waiting Time Constraints

To ensure service quality, mother stations must process charging demands promptly. Waiting time constraints for both demand types are set:

$$W_e \le W_{max/e} \quad (3\text{-}14)$$

$$W_n \le W_{max/n} \quad (3\text{-}15)$$

Where $W_{max/e}$ and $W_{max/n}$ are the maximum permissible waiting times for emergency and routine demands, respectively.

(5) MCR Operational Constraint

To ensure MCRs can cover emergency demands without themselves becoming stranded:

$$G_{\mathrm{r}} l_{(k,k+1)} + \left(S_{\mathrm{soc,o}} - S_{\mathrm{soc,c}}\right) F_{\mathrm{V}} \le F_{\mathrm{R}} \quad (3\text{-}16)$$

This constraint ensures that an MCR, after serving an emergency demand requiring energy , has sufficient remaining charge in its own battery to travel the distance $l_{(k,k+1)}$ to the next mother station $k+1$ for replenishment. G_{r} is the MCR's energy consumption per unit distance. $S_{\mathrm{soc,o}}$ and $S_{\mathrm{soc,c}}$ are as defined previously.

4.3 Solving the Multi-Objective Optimization Model

Given the multi-objective, high-dimensional, and strongly constrained nature of the charging network planning problem, this paper proposes an improved Non-dominated Sorting Genetic Algorithm II (NSGA-II) with elite preservation. The detailed flowchart is shown in **Figure 2**, and the specific steps are as follows:

Step 1. Population Initialization: Generate an initial population randomly to maintain diversity. Each individual's chromosome encodes a complete solution.

Step 2. Fitness Evaluation: Evaluate each individual's objective values in parallel. The evaluation process involves calculating coverage based on the MCM logic and verifying service capability by computing system performance metrics (waiting times, load rates) using the queuing model from Section 3.2 to check constraint satisfaction.

Step 3. Elite Selection - Non-dominated Sorting and Crowding Distance Calculation: Apply the fast non-dominated sorting algorithm to rank individuals into different Pareto fronts. For individuals within the same front, calculate the crowding distance. Elite individuals (those in the best fronts) are identified for preservation.

Step 4. Evolutionary Operations: Generate offspring through genetic operators.

Crossover: Apply multi-point crossover on selected parent individuals to produce new solutions.

Mutation: Apply directed mutation to enhance local search and maintain population diversity.

Step 5. Offspring Evaluation: Evaluate the fitness values of the newly generated offspring in parallel, using the same criteria as in Step 2.

Step 6. Population Recombination: Combine the elite individuals from the parent population (identified in Step 3) with the newly generated offspring population. To form the new parent population for the next generation, select individuals based on the following hierarchy:

1. Lower (better) non-dominated front rank is preferred.
2. Within the same front, a larger crowding distance is preferred (to promote diversity).

Step 7. Termination Check: Terminate the algorithm if the maximum number of generations (iterations) is reached. Otherwise, return to Step 3.

Step 8. Solution Selection: Based on the final Pareto-optimal front obtained by the NSGA-II algorithm, select the final decision solution. A decision-making method can be applied to choose the most suitable compromise solution from the non-dominated set.

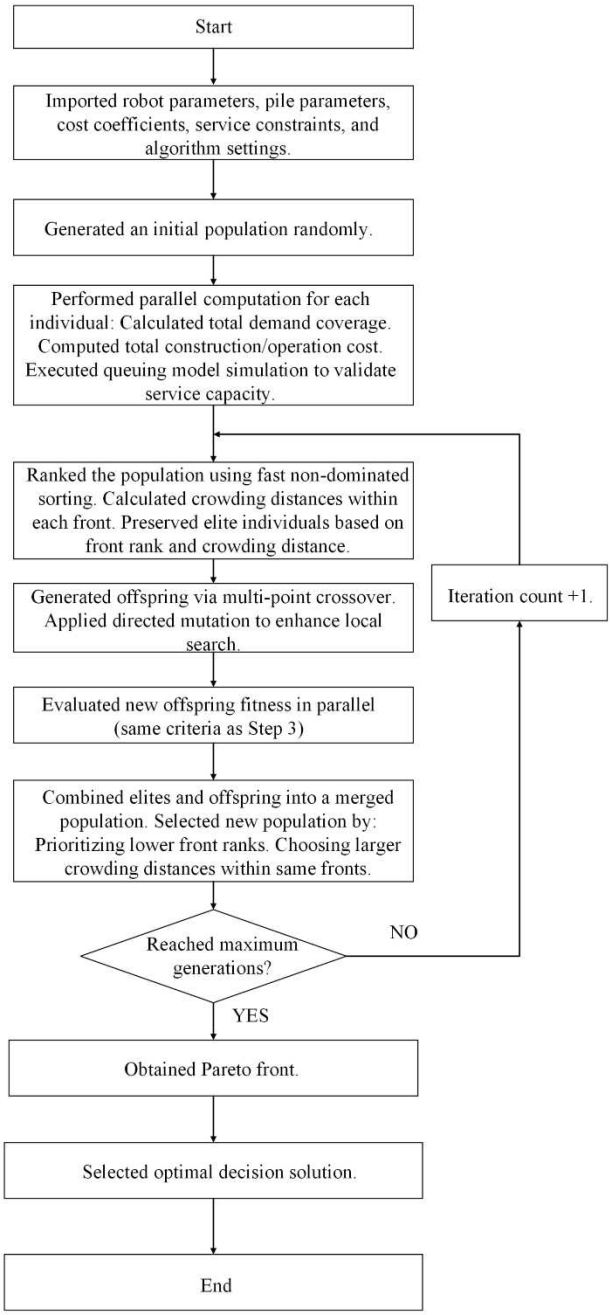


Figure 2 Flowchart of NSGA-II

5 Case Study

5.1 Case Scenario Setup

This study assumes a specific highway segment, as illustrated in **Figure 3**. The figure depicts a bidirectional highway segment containing several interchanges. Points A and E represent some of the highway entrances, while D and H represent some of the exits. Between points B and C on this segment, there exist numerous interchanges similar to B-G and C-F, connecting the two directional carriageways to allow EVs and MCRs to adjust their travel direction. This numerical example selects the B-C-F-G segment with a total length of 1000

km, constituting a portion of the highway network. MCRs operate and provide services within this network. To ensure a dynamic balance in the number of MCRs at each station over the long term, MCRs can return from downstream segments to upstream segments via interchanges, achieving resource rebalancing across the entire line. Combining with the real-world condition where service areas are typically built every 50-100 km on highways, candidate sites are selected at 60 km intervals. The typical daily traffic volume for the highway is shown in **Figure 3** [22]. It is assumed that all vehicles entering this highway are Battery Electric Vehicles (BEVs). The traffic flow in each time period consists of three battery capacity types: 30 kWh, 60 kWh, and 90 kWh. For each battery capacity, EVs are further divided into sedans and SUVs. The distribution of each vehicle type is random. The initial battery State of Charge (SOC) follows a normal distribution N(0.5, 0.204) [26]. EV travel speed follows a uniform distribution U(90, 120) km/h. The energy consumption per kilometer for each vehicle is derived from the energy consumption model. The MCR's battery capacity is 300 kWh, its travel speed is 120 km/h, and its energy consumption per kilometer is 0.2 kWh/km.

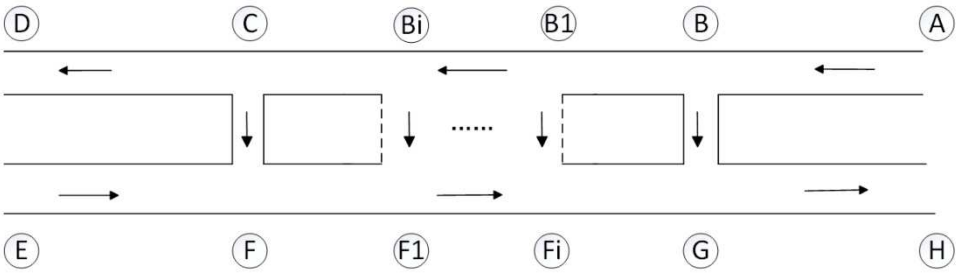


Figure 3 Schematic diagram of the road segment

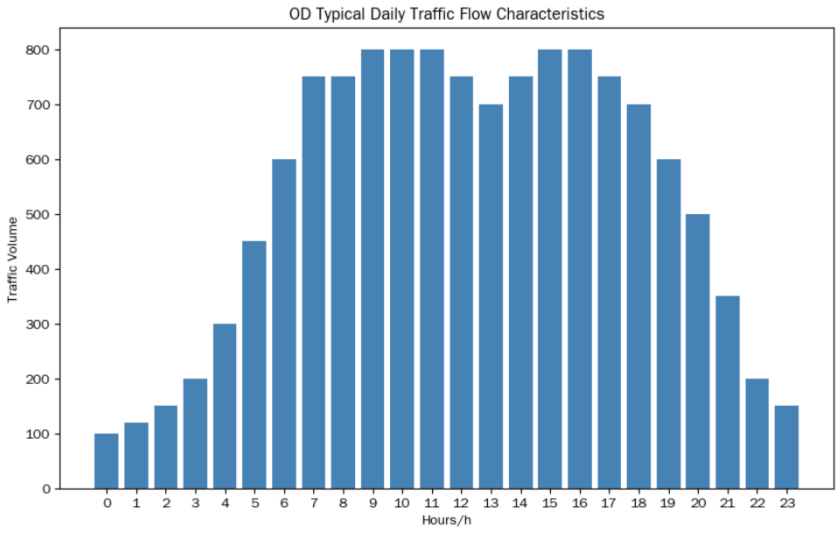


Figure 4 Daily traffic volume diagram

5.2 Simulation Results

（1） Charging Demand Prediction Results

Analysis based on the EV energy consumption model indicates that under both routine

and emergency conditions, the energy consumption of SUVs is significantly higher than that of sedans, as shown in **Figure 5**. Furthermore, the study finds that EV energy consumption shows a continuous increasing trend with rising speed, as depicted in **Figure 6**.

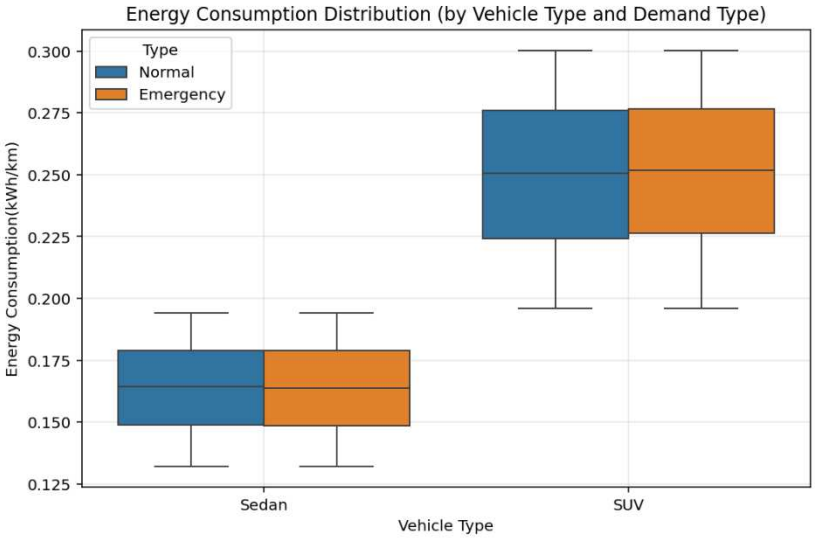


Figure 5 Comparison of energy consumption distribution

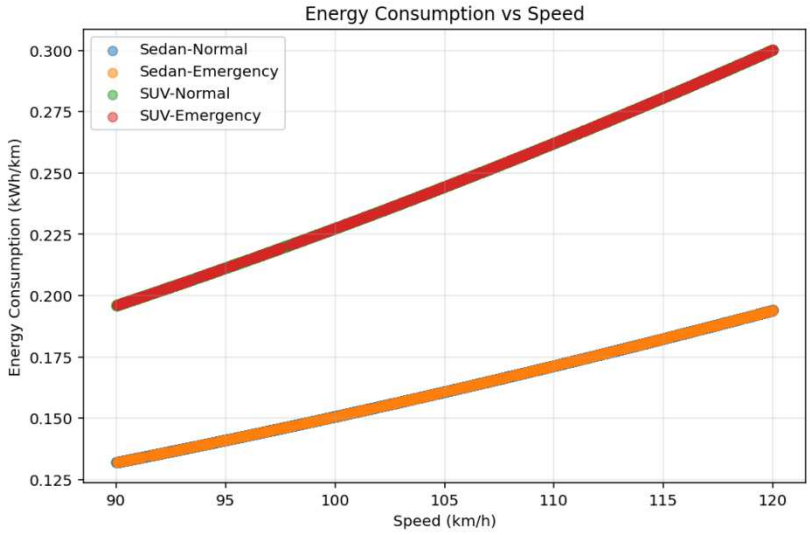


Figure 6 Relationship between energy consumption and speed

Based on traffic flow, EV parameters, and the energy consumption model, the routine and emergency charging demands on the highway are predicted. The results are shown in **Figure 7**. Here, the X-axis represents the demand generation location, the Y-axis represents time, the Z-axis represents energy demand (kWh), and color intensity reflects demand magnitude. Analysis shows that during the early morning hours (0–5 AM), traffic flow is low, resulting in fewer emergency demands, while routine demand maintains a relatively high level throughout.

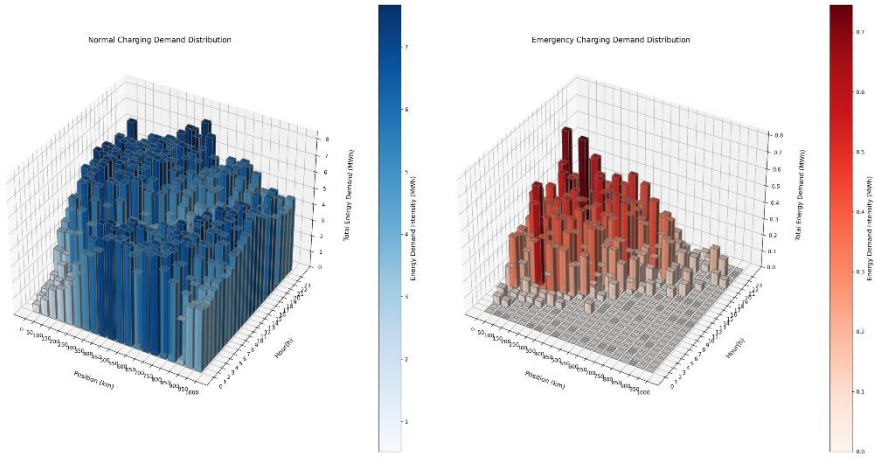


Figure 7 Prediction results of charging demand

（2） Mother Station Siting Results

The charging demand prediction results obtained via Monte Carlo simulation are used as input. Based on the multi-objective optimization model for siting dual-use MCR mother stations, the solution is obtained using the improved Non-dominated Sorting Genetic Algorithm II (NSGA-II). Relevant parameters are listed in **Table 1** and **Table 2** below.

TABLE 1 Parameter settings of the NSGA-II algorithm

NSGA-II Parameter	Value
Population Size	500
Maximum Generations	300
Crossover Probability	0.7
Mutation Probability	0.3
Number of Elite Preserved	100

TABLE 2 Simulation parameter settings

Parameter	Value	Unit	Parameter	Value	Unit
$S_{soc,e}$	N(0.5,0.204)	kwh	α	0.5	
$S_{soc,c}$	U(0.1,0.3)	kwh	v	U(90,120)	km/h
$S_{soc,o}$	U(0.6,0.9)	kwh	v_r	120	km/h
F_{V1}	30	kwh	T	20	year
F_{V2}	60	kwh	β	0.1	
F_{V3}	90	kwh	$c_{cs,m}$	200	10^4 CNY
F_r	200	kwh	c_r	20	10^4 CNY
η_t	90%		c_c	5	10^4 CNY
η_c	90%		K_{rmin}	1	
G_V	0.16	kWh/km	K_{rmax}	25	
G_r	0.2	kWh/km	K_{cmin}	1	
P_e	350	kW	K_{cmax}	30	
P_n	200	kW	ρ_{max}	1	

θ	3%		$W_{\max/n}$	30	min
μ_{roll}	0.01		g	9.8	m/s²
m_{SUV}	1900	kg	m_{Sedan}	1600	kg
ρ_{air}	1.225	kg/m³	$f_{congestion}$	1.2	
$C_{d/SUV}$	0.35		$C_{d/Sedan}$	0.25	
$W_{max/e}$	20	min	A_{Sedan}	2.5	m²
A_{SUV}	3	m²			

The Pareto frontier obtained from solving the model is shown in **Figure 7**. The results indicate that as the investment cost increases, the charging demand coverage rate shows a trend of increasing at a decelerating rate. When the annual cost increases from 5 million CNY to 6 million CNY, the growth in coverage is extremely limited. When the cost reaches 6.33 million CNY, the coverage rate exceeds 95%.

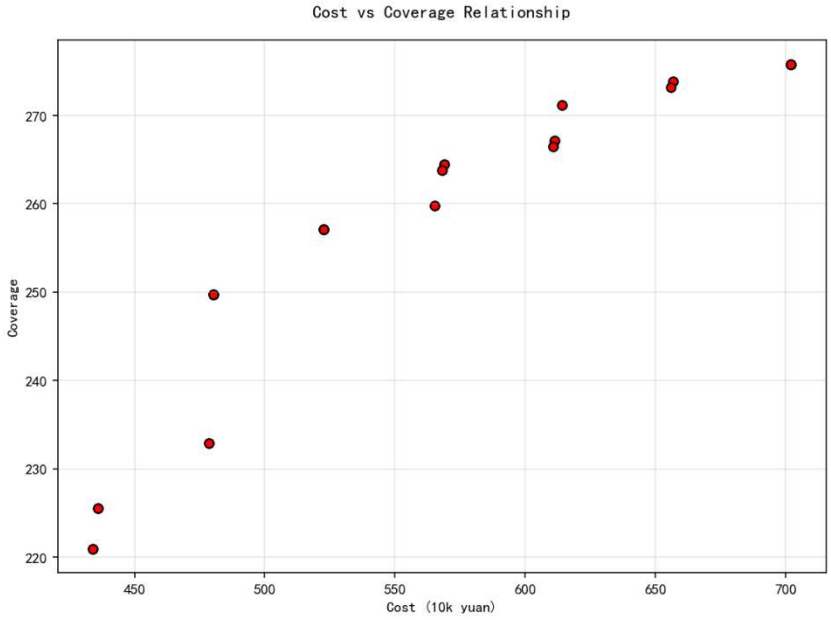


Figure 8 Pareto front of mother station planning schemes

From the investor's perspective, when construction funds are limited, priority should be given to a plan that covers the vast majority of charging demand. Therefore, considering only the maximization of charging demand coverage, the plan with an investment of 6.33 million CNY for mother stations represents a preferable choice, as its demand coverage exceeds 95%. This plan involves the construction of 16 mother stations, including 54 MCRs and 84 charging piles. There are 38 emergency demand points, of which 33 are covered, and 115 routine demand points, all of which are covered. The corresponding siting scheme is detailed in **Table 3**.

TABLE 3 Mother station location planning schemes

Mother Station Location (km)	Number of MCRs	Number of Charging Piles	Mother Station Location (km)	Number of MCRs	Number of Charging Piles
60	5	1	540	5	6
120	3	4	600	3	3
180	3	9	660	1	15

240	1	4	720	3	3
300	6	5	780	6	13
360	2	3	840	3	3
420	5	1	900	1	3
480	5	7	960	2	4

In actual highway operations, charging demands across different times and segments exhibit variation due to the coupling of travel behaviors. Combining with the charging demand simulation results in Figure 6, it is evident that routine demand consistently remains at a high level. Therefore, in areas with high charging demand, the configuration of MCRs and charging piles is greater. For emergency demand, locations with higher emergency demand at 300 km, 420 km, 540 km, and 780 km are equipped with a larger number of MCRs. In summary, the configuration of charging robots and charging piles, as well as the station locations derived from the System Three-Stage Dynamic Planning Theory (STSDLAP), match the charging demand pattern. The planning results are more economical and reasonable, effectively meeting the routine and emergency charging needs of EVs on the highway.

5.3 Sensitivity Analysis

The spacing between candidate sites has a significant impact on the optimization results of the MCR mother station siting model. Changes in spacing alter the coverage capability of each station for routine and emergency demands, thereby affecting site selection and equipment configuration. It also adjusts the travel time for robots to reach emergency points, which relates to service quality. Therefore, a sensitivity analysis is conducted on the distance setting of candidate sites, simultaneously adjusting the MCR's travel speed accordingly. The siting results for MCR mother stations are compared for candidate site intervals ranging from 30 km to 90 km, as shown in **Table 4**.

TABLE 4 Comparative results of location planning with different spacing

Site Interval (km)	Total Number of Mother Stations	Total Number of MCRs	Total Number of Charging Piles	Number of Emergency Demands Covered	Number of Routine Demands Covered	Total Cost (10k CNY)
90	11	23	26	31	110	386.4
80	12	31	44	32	114	446
70	14	32	52	32	115	512
60	16	54	84	33	115	633
50	17	66	125	35	115	721.9
40	21	60	111	38	115	811.5
30	24	85	170	38	115	1003

According to the results in Table 4, as the candidate site interval decreases, the number of candidate sites, the number of constructed stations, and the configuration of charging piles and MCRs all increase correspondingly, leading to a rise in mother station planning costs. Although the charging demand coverage rate improves, the growth gradually tends to saturate. From an economic perspective, the planning scheme with a 60 km site interval is recommended as the priority choice, which also aligns well with the existing spacing of highway service areas.

6 CONCLUSIONS

This study constructed a three-stage dynamic planning theoretical framework encompassing "demand prediction, performance evaluation, and siting optimization." This framework systematically addresses the modeling and optimization challenges of coordinated dispatch between Mobile Charging Robots (MCRs) and fixed charging piles for integrated routine and emergency scenarios on highways. It effectively enhances emergency handling

capabilities and compensates for the service gaps of fixed infrastructure. Through a scientific siting layout of MCR mother stations, it ensures the minimal construction/operation cost and maximal demand coverage.

Stage 1: By integrating an EV travel model, an energy consumption model, and Monte Carlo simulation, this stage comprehensively considers both daily patterns and the randomness of incidents, overcoming the deficiencies of traditional simplified energy consumption models and inadequate emergency demand prediction.

Stage 2: Based on M/M/C queuing theory, this stage introduces a non-preemptive priority dispatch mechanism. Under constrained resources, it guarantees emergency service response within 30 minutes, enabling the quantitative evaluation of service quality.

Stage 3: A multi-objective siting model was established, aiming at minimizing construction cost and maximizing coverage for both routine and emergency demands. Practical constraints such as load rates and waiting times were embedded. An improved NSGA-II algorithm was employed for solution. The optimal scheme derived from Pareto frontier analysis demonstrates that, on a 1000-kilometer highway segment, it can achieve emergency response within 30 minutes and meet over 95% of the total charging demand.

While the current research has yielded theoretical and practical results, there remains room for further development. Critical issues in practical application, such as the energy replenishment mechanism for MCRs, network optimization strategies, and their synergy modes with Intelligent Transportation Systems, have not been explored in depth. Furthermore, costs associated with MCR empty mileage, additional energy consumption, and time occupancy were not considered. Future research should focus on continuously optimizing the EV energy consumption prediction model by integrating multi-source heterogeneous data, deepening the study of cooperative optimization between MCRs, Internet of Vehicles, and smart grids, and exploring intelligent and dynamic siting and dispatch strategies. These efforts aim to construct a more comprehensive theoretical system and practical pathway for the high-quality development of highway charging infrastructure.

Declaration

Conflicting Interests

The authors have no competing interests to declare that are relevant to the content of this article.

Funding

This study was funded by Philosophy and Social Science Foundation of China: China-Russia Trade Western Corridor Economic Corridor: A Study on Trade, Industry and Corridor Capacity (grant 20BGL015).

AUTHOR CONTRIBUTIONS

The authors confirm contribution to the paper as follows: study conception and design: Hao Jiang, Hailing Wang; data collection: Hao Jiang; analysis and interpretation of results: Hao Jiang, Hailing Wang; draft manuscript preparation: Hao Jiang. All authors reviewed the results and approved the final version of the manuscript.

Data Availability statement

The datasets used or analysed during the current study available from the corresponding author on reasonable request.

REFERENCES

1. HU Dandan, KOU Jingze. Site selection, capacity determination, and reconstruction optimization strategy for electric vehicle charging/swapping stations[J]. Journal of Chongqing University of Technology(Natural Science),2024,38(05):30-37. (in Chinese)

2. ZHANG Meixia, FU Yulin, YANG Xiu. Planning of charging and battery swappin g facilities based on spatio-temporal distribution of charging and battery swapping dem and of electric vehicles[J]. Journal of ctric Power Science and Technology,2025,40(01): 126-137.DOI:10.19781/j.issn.1673-9140.2025.01.013. (in Chinese)

3. Li N, Chen S, Zhang Z. A queuing model based metamodel simulation optimization for capacity design of integrated battery swapping and charging station[J]. Computers & Industrial Engineering, 2025,206111148-111148.

4. Liu B, Gao X, Wang Y, et al. Co-construction strategy of battery swapping stations and charging piles in China[J]. Transport Policy,2025,16956-73.

5. Hua L, Dongmin S, Bongju J. Electric vehicle charging scheduling with mobile charging stations[J]. Journal of Cleaner Production,2024,434140162-.

6. Tang P, He F, Lin X, et al. Online-to-offline mobile charging system for electric vehicles: Strategic planning and online operation[J]. Transportation Research Part D,2020,87

7. YANG Yazao, BIN Tao. Electric Vehicle Centralized Charging Station Siting and Capacity Modeling[J]. Journal of Transportation Systems Engineering and Information Technology, 2024,24(03):204-212. DOI:10.16097/j.cnki.1009-6744.2024.03.020. (in Chinese)

8. CAO Mukun, WANG Yicheng, LIU Xinlong, et al. Research on location model o f new energy vehicle charging station driven by trajectory data[J/OL]. Control and De cision,1-9[2025-06-27]. https://doi.org/10.13195/j.kzyjc.2024.0929. (in Chinese)

9. JIANG Changxu, LU Yuejun, LIN Zheng, et al. Layout Planning Of Expressway Charging Stations Considering Interaction Between Charging Stations[J]. Acta Energiae Solaris Sinica,2025,46(04):11-21. DOI:10.19912/j.0254-0096.tynxb.2023-2042. (in Chinese)

10. Chowdhury R, Mishra P, Mathur D H. Optimal scheduling of mobile and stationary electric vehicle charging stations in a distribution system with stochastic loading[J]. Energy,2025,326136305-136305.

11. DAI Yang, GUO Shuang, ZHANG Cong. Highway Charging Station Siting an d Sizing Model for Intercity Travel[J/OL]. Industrial Engineering and Management,1-20 [2025-06-03]. https://kns-cnki-net.webvpn.xju.edu.cn:8040/kcms/detail/31.1738.T.20250227. 1626.017.html. (in Chinese)

12. Shi Ruifeng, Chang Tai, He Zhe, et al. Research on Planning Method for Photovoltaic-Storage-Charging Integrated Electric Vehicle Charging Stations[J]. Acta Energiae Solaris Sinica,2025,46(05):109-118. DOI:10.19912/j.0254-0096.tynxb.2024-0023. (in Chinese)

13. ZHANG Wenhui, SU Jiaqi, HA Zihong, et al. Location and Capacity Optimization Model of Battery-Swapped Electric Bus Charging Station[J]. Journal of South China University of Technology(Natural Science Edition),2023,51(10):126-134. (in Chinese)

14. Wang W, Liu Y, Fan X, et al. Optimization of Charging Station Capacity Based on Energy Storage Scheduling and Bi-Level Planning Model[J]. World Electric Vehicle Journal,2024,15(8):327-327.

15. YANG Jieqing, JIANG Xiaoxue, ZHAO Kequan. Multi-objective Optimization Method of Location and Capacity Determination Problems of Highway Charging Stations[J]. Journal of Chongqing Normal University(Natural Science),2021,38(01):11-21. (in Chinese)

16. LIU Hong, LI Rong, GE Shaoyu, et al. Multi-objective Planning of Electric Vehicle Charging Stations on Expressway Based on Dynamic Traffic Flow Simulation[J]. Automation of Electric Power Systems, 2015,39(24):56-62+79. (in Chinese)

17. ZHANG Zhaolei, HAO Wei, LI Hao, et al. Optimized Deployment of Charging Piles Based on Extended Traffic Equilibrium in Highway[J]. China Journal of Highway and Transport,2024,37(04):61-71. DOI:10.19721/j.cnki.1001-7372.2024.04.006. (in Chinese)

18. Cui S, Yao B, Chen G, et al. The multi-mode mobile charging service based on electric vehicle spatiotemporal distribution[J]. Energy,2020,198(prepublish):117302-117302.

19. Huasheng L, Yu L, Chongyu Z, et al. Electric Vehicle Charging Station Location Model considering Charging Choice Behavior and Range Anxiety[J]. Sustainability,2022, 14(7):4213-4213.

20. LI Jiapei, XIE Chi. A Metanetwork-based Optimization Approach to Locating Charging Stations for Electric Vehicles in Highway Networks[J]. China Journal of Highway and Transport,2024,37(04):1-13. DOI:10.19721/j.cnki.1001-7372.2024.04.001. (in Chinese)

21. LI Jianxia, ZHAO Feng, GAO Fengyang. Hierarchical Optimization for Capacity of PV-integrated EV Charging Station on Expressway Based on HOMER and Tabu Algorithm[J]. Journal of Power Supply,2022,20(06):127-136. DOI:10.13234/j.issn.2095-2805.2022.6.127. (in Chinese)

22. Ge Shaoyun, Zhu Linwei, Liu Hong, et al. Optimal Deployment of Electric Vehic le Charging Stations on the Highway Based on Dynamic Traffic Simulation[J]. Transac tions of China Electrotechnical Society,2018,33(13):2991-3001. DOI:10.19595/j.cnki.1000 -6753.tces.170608. (in Chinese)

23. Ömer Kaya. Photovoltaic mobile charging station for green infrastructure: A data-driven case study[J]. Urban Climate,2025,60102358-102358.

24. GE Shaoyun, ZHOU Hao, LIU Hong, et al. Coordinated Planning for Highway Charging Stations and Rest Area Considering the Impact of Traffic Accidents[J]. Proceedings of the CSU-EPSA,2019,31(03):1-8. DOI:10.19635/j.cnki.csu-epsa.000152. (in Chinese)

25. DONG X H,MU Y F,JIA H J,et al. Planning of fast EV charging stations on a round freeway［J］. IEEE Transactions on Sustainable Energy,2016,7(4):1452-1461.

26. GE Shaoyun, FENG Liang, LIU Hong, et al. Planning of charging stations on highway considering power distribution and driving mileage[J]. Electric Power Automation Equipment,2013,33(07):111-116. (in Chinese)